A-6-01 (Invited) Extended Abstracts of the 2020 International Conference on Solid State Devices and Materials, VIRTUAL conference, 2020, pp51-52

Metal-Assisted Solid Phase Crystallization of Vertical Si Channel in 3D Flash Memory

Hidenori Miyagawa[1], Haruka Kusai[1], Riichiro Takaishi[1], Tomoya Kawai[1], Yuuichi Kamimuta[1], Toshiya Murakami[1], Keiko Ariyoshi[1], Takanori Asano[1], Masakazu Goto[1], Makoto Fujiwara[1], Yuichiro Mitani[1], Tomoyuki Obu[2] and Hideaki Aochi[1]

[1]Institute of Memory Technology Research & Development, Kioxia Corporation, Yokkaichi, Japan,
E-mail: hidenori.miyagawa@kioxia.com
[2]Western Digital Corporation, Yokkaichi, Japan,

Abstract

In order to improve the channel conductance of 3D flash memory, we successfully fabricated monocrystalline Si channel from amorphous Si by applying metal induced lateral crystallization technology. The 3D flash memory equipped with this technology demonstrated superior electrical characteristics and reduced variation compared to conventional devices with poly-Si channel.

1. Introduction

One approach to enhance the bit density of 3D flash memory is the increase of the number of vertically stacked word lines. However, the highly-stacked structures cause a performance degradation due to increased channel resistance and cell Vth variation which derived from grain boundaries in poly-Si [1].

Hence, we focused on the metal induced lateral crystallization (MILC), which is well-known for improving channel conductance in thin film transistors (TFTs) [2, 3]. Metal thin film such as Ni or Pd is deposited on the source / drain regions and metal thin film is transformed into metal silicide by annealing at low temperature. Then, the solid-phase epitaxy proceeds following the movement of the metal silicide tip, and the growth of crystal grains is accelerated.

In this work, we applied the MILC technology to thin Si channel film inside the vertical memory holes in the 3D flash memory [4]. The physical analysis and the evaluation of electrical characteristics were carried out.

2. Application of Metal-Assisted Crystallization to 3D Flash Memory

In this work, MILC process applied to thin Si film in vertical memory holes is represented as “metal-assisted solid-phase crystallization (SPC) process”. The vertical memory process to which we applied metal-assisted SPC is shown in Fig. 1. After forming the vertical memory holes, ONO stack and amorphous Si (a-Si) film ($t_{a\text{-}Si}$= 20nm) were deposited, and subsequently dielectric filler (SiO_2) was buried in the holes. SiO_2 and a-Si at the top of memory holes were removed and the surface of "macaroni-shaped" a-Si was exposed. Then, thin Ni film (~10nm) was deposited. After Ni silicide formation and excess Ni removal using SPM (Sulfuric Acid Hydrogen Peroxide Mixture), monocrystalline Si channel was grown by crystallization annealing.

Fig. 2 shows the snap shots of in-situ TEM image of the vertical memory hole during metal-assisted SPC. In the case of thin Si channel in the vertical holes, it was clearly observed

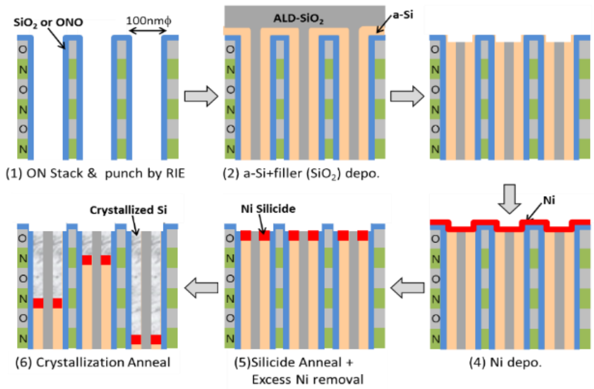

Fig. 1 Application of metal-assisted solid-phase crystallization for vertical holes (Ref. 4, @2019 IEEE).

that Ni silicide exists at growing tip and the crystal Ni silicide moves along Si channel crystallization. As previously reported [5], in the metal-assisted SPC, the crystallization proceeds by simultaneously putting Si atoms in a-Si into Ni silicide at a-Si / NiSix interface and emitting Si atoms behind Ni silicide at c-Si / NiSix interface.

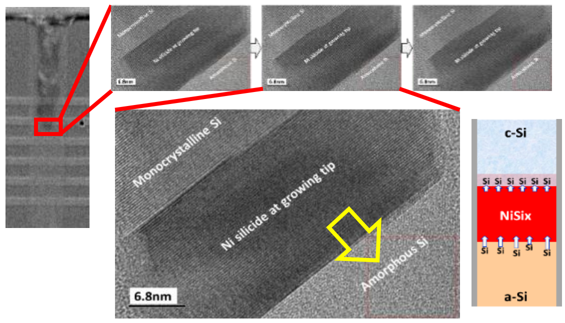

Fig. 2 Snap shots of in-situ TEM image of growing tip for metal-assisted SPC (Ref. 4, @2019 IEEE). It was observed that the epitaxial Ni silicide moves toward amorphous Si and the monocrystalline Si follows.

Fig. 3 shows the site-specific nano beam diffraction two-dimensional imaging (NBD-2DI) of the vertical memory holes with the poly-Si channel (Fig. 3(a)) and that with the metal-assisted SPC channel (Fig. 3(b)). The NBD-2DI measurement technique is able to characterize the channel crystallinity obtained from analysis of diffraction patterns [6]. The crystallization conditions were 850ºC 30 minutes for the poly-Si channel, and 550ºC 4 hours for the metal-assisted SPC channel, respectively. In the case of the poly-Si channel, the NBD patterns at the points of #2-#7 are different, though

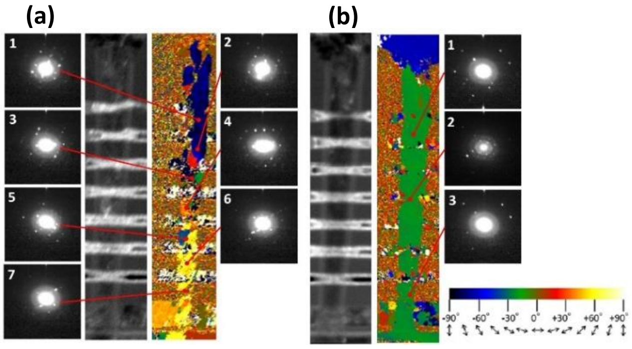

Fig. 3 NBD-2DI images for crystallinity obtained from diffraction patterns, (a) poly Si channel, and (b) metal-assisted SPC Si channel (Ref. 4, @2019 IEEE). The intensity in each position represents the intensity of center beam in each NBD pattern. NBD pattern for each point are also shown. In the color map, the angle of the diffraction spot is measured and displayed for each point in the NBD mapping. The reference angle is set to 0° in the [001] direction of the Si substrate.

the similar NBD patterns are observed at the points of #1 and #2. This result indicates the poly-Si channel consists of randomly aligned grains with various size.

On the other hand, for the metal-assisted SPC channel, NBD patterns at the points of #1-#3 are almost the same, indicating the metal-assisted SPC channel is identified to be a single crystal.

The device characteristics of the metal-assisted SPC channel were directly compared to those of the poly-Si channel. The 7-layer tungsten-replaced word line test vehicle with 1μm-depth and 100nmΦ vertical memory cells was utilized for analyzing the device characteristics. The respective V_G-I_{cell} data of randomly extracted 50 devices are shown in Fig. 4. The improvement for the metal-assisted SPC channel was distinctly observed compared to the poly-Si channel. I_{cell}, subthreshold slope (S.S.), and variability can be dramatically improved by metal-assisted SPC process. The correlation between S.S. and Vth for the devices with the poly-Si channel and the metal-assisted SPC channel is shown in Fig. 5. The data plots of the metal-assisted SPC (monocrystalline channel) are separated from those for the poly-Si channel. The data for the poly-Si channel scatters widely, while the data for the metal-assisted SPC channel gathers in the region of low

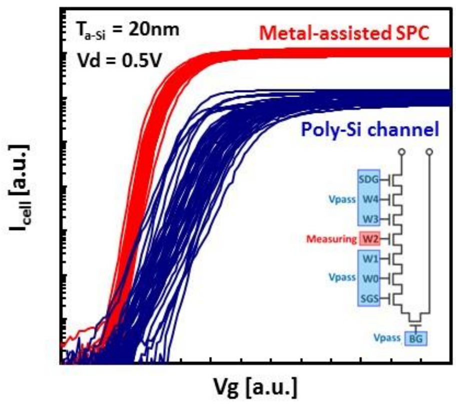

Fig. 4 V_G-I_{cell} characteristics for poly-Si channel, and metal-assisted SPC channel (Ref. 4, @2019 IEEE).

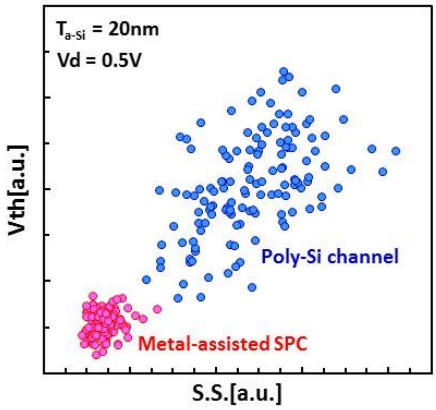

Fig. 5 Correlation between sub-threshold slope (S.S.) and V_{th} for poly-Si channel and metal-assisted SPC channel (Ref. 4, @2019 IEEE).

S.S. and low Vth. This result also indicates that traps due to defects in Si channel are eliminated by realizing monocrystalline through metal-assisted SPC process. In addition, we have confirmed that the data retention, the endurance, the program / erase characteristics and the memory window of metal-assisted SPC channels are almost consistent with those of poly-Si channels. Based on these results, it can be concluded that the metal-assisted SPC process gives us superior cell current and uniformity without influence on both memory performance and reliability in 3D flash memory.

3. Conclusions

We successfully fabricated monocrystalline Si channel from amorphous Si via nickel silicide by applying MILC technology to Si thin film in the vertical memory holes. Monocrystalline Si growth along Ni silicide tip moving was directly observed by in-situ TEM and the grown channel by the metal-assisted SPC was determined as single crystal of Si by NBD analysis. Moreover, superior cell current and uniformity was achieved and the metal-assisted SPC process has no influence on the memory performance and reliability. This technology is the one of the promising breakthroughs for the performance improvement of highly-stacked 3D flash memories.

Acknowledgements

The authors gratefully acknowledge the contributions of Drs. T. Ishida, N. Kuge, Y. Moriyama, T. Tezuka, In addition, the authors thank Drs. M. Saitoh, M. Koyama, T. Numata, S. Kawanaka and T. Maruyama for their encouragement and support.

References

[1] Y. Fukuzumi et al.:*Tech Dig IEEE Int. Electron Device Meeting* (2007) 449.
[2] S.-W. Lee et al.: Appl. Phys. Lett. **66** (1995) 1671.
[3] S.-W. Lee et al.: IEEE Electron Dev. Lett. **17** (1996) 160.
[4] H. Miyagawa et al.: *Tech Dig IEEE Int. Electron Device Meeting* (2019) 650.
[5] G. Z. Radnoczi et al.: J. Appl. Phys. **119** (2016) 065303.
[6] T. Asano et al.: *IEEE Int. Reliability Physics Symposium (IRPS)* (2017) 5C-2